Photoinduced Heterocyclic Ring-Opening of Furfural: Distinct Open-Chain Product Identification by Ultrafast X-ray Transient Absorption Spectroscopy

Aditi Bhattacherjee,[1,2,5] Kirsten Schnorr,[1,2,6] Sven Oesterling,[3] Zheyue Yang,[1,2] Tian Xue,[1,2] Regina de Vivie-Riedle,[3] and Stephen R. Leone*[1,2,4]

[1] *Department of Chemistry, University of California, Berkeley, California 94720, USA*
[2] *Chemical Sciences Division, Lawrence Berkeley National Laboratory, Berkeley, California 94720, USA*
[3] *Department of Chemistry, Ludwig-Maximilians-Universität München, München 81377, Germany*
[4] *Department of Physics, University of California, Berkeley, California 94720, USA*

Submitted to

Journal of the American Chemical Society

AUTHOR EMAIL ADDRESS: aditibhattacherjee@gmail.com, schnorr@posteo.de, sven.oesterling@cup.uni-muenchen.de, yangzy_sh@berkeley.edu, xuetian2016@berkeley.edu, regina.de_vivie@cup.uni-muenchen.de, srl@berkeley.edu

Abstract

The ultraviolet-induced photochemistry of five-membered heterocyclic rings often involves ring opening as a prominent excited-state relaxation pathway. The identification of this particular photoinduced mechanism, however, presents a challenge for many experimental methods. We show that femtosecond X-ray transient absorption spectroscopy at the carbon K-edge (~284 eV) provides core-to-valence spectral fingerprints that enable the unambiguous identification of ring-opened isomers of organic heterocycles. The unique differences in the electronic structure between a carbon atom bonded to the oxygen in the ring versus a carbon atom set free of the oxygen in the ring-opened product are readily apparent in the X-ray spectra. Ultrafast ring-opening via C-O bond fission occurs within ~350 fs in 266-nm-photoexcited furfural, as evidenced by fingerprint core (carbon 1s) electronic transitions into a non-bonding orbital of the open-chain carbene intermediate at 283.3 eV. The lack of recovery of the 1sπ^* ground-state depletion in furfural at 286.4 eV indicates that internal conversion to the ground state is a minor channel. These experimental results, augmented by recent advances in the generation of isolated attosecond pulses at the carbon K-edge, will pave the way for probing ring-opened conical intersection dynamics in the future.

Introduction

Five-membered heterocyclic organic rings such as furan are key building blocks in polymers,[1,2] molecular optoelectronics,[3,4] pharmacological agents,[5] atmospheric compounds[6,7] and fuels.[8,9] As such, the energy relaxation pathways available to these cyclic molecules upon electronic excitation are of great interest.[10] Ultraviolet excitation near the absorption maximum populates a $^1\pi\pi^*$ (S_2 at the Franck-Condon point, FC) electronically-excited state. The ensuing photochemistry is notably mediated by a conical intersection (CI) with a higher-lying $\pi\sigma^*$ state (labelled S_3 in Figure 1) that can lead to a carbon-heteroatom bond fission, i.e. ring-opening (o) can occur via promotion of an electron from a π-bonding orbital to a σ^*_{CO} anti-bonding orbital (Figure 1b). This pathway involves non-adiabatic passage of the excited molecule via two successive CIs, an initial $S_3(^1\pi\sigma^*)/S_2(^1\pi\pi^*)$ CI close to the FC region and a subsequent $S_3(^1\pi\sigma^*)/S_0(\pi^2n^2)$ CI_O. An alternative route of non-adiabatic coupling to the ground-state involves a particular nuclear distortion known as ring-puckering (p) in S_2, where the molecule loses planarity and the H atom in the α- or δ-position with respect to the heteroatom is bent (Figure 1a). In this case, the excited molecule evolves on a single electronic state surface ($^1\pi\pi^*$, S_2), which is the initial photoexcited state, before arrival at a direct CI_P with the ground state.

Furfural (or furan-2-carbadehyde, Figure 1) is the simplest aldehyde derivative of furan, it is a potential biomass-derived biofuel, and it is used extensively in agrochemical, petroleum, plastics, and pharmaceutical industries.[11,12] The photodynamics of furfural can be contrasted with its base compound, furan. Time-resolved photoelectron imaging studies of furan, using both 4.7 eV and 7.8 eV probe pulses, indicated that ring puckering is the predominant pathway.[13,14] This is inferred from the temporal invariance of the anisotropy parameter at each observed photoelectron kinetic energy, indicating that the electronic character does not change upon excited state relaxation. In contrast, another femtosecond photoelectron imaging study[15] with 800-nm multiphoton ionization as a probe revealed biexponential decay kinetics of photoexcited furan, attributed to an initial $S_2 \rightarrow S_1$ internal conversion and subsequent decay of vibronic S_1 to the formation of α- and β-carbenes, also reported to be formed in furan pyrolysis.[16] A recent time-resolved photoelectron study reports the effect of aldehyde substitution on the photoinduced relaxation dynamics of furan, i.e. parent compounds

furfural and β-furfural, using a high-intensity, two-photon ionization probe.[17] The relaxation dynamics of furfural are found to be slowed down (~ hundreds of femtoseconds) in comparison to furan (sub-100 fs) and additionally involve a deactivation pathway via a $n\pi^*$ state (n being the non-bonding orbital of the carbonyl oxygen).[17] In that same work, CASSCF dynamics of furan and furfural indicate trajectories of both the ring opening and puckering channels, with a clear preference for ring-opening.[17] Here, we use X-ray transient absorption at the carbon K-edge to identify the ring-opened photoproduct generated by the photoexcitation of furfural, whose ultraviolet absorption spectrum is conveniently accessed by the third harmonic (266 nm) of a Ti:sapphire laser.

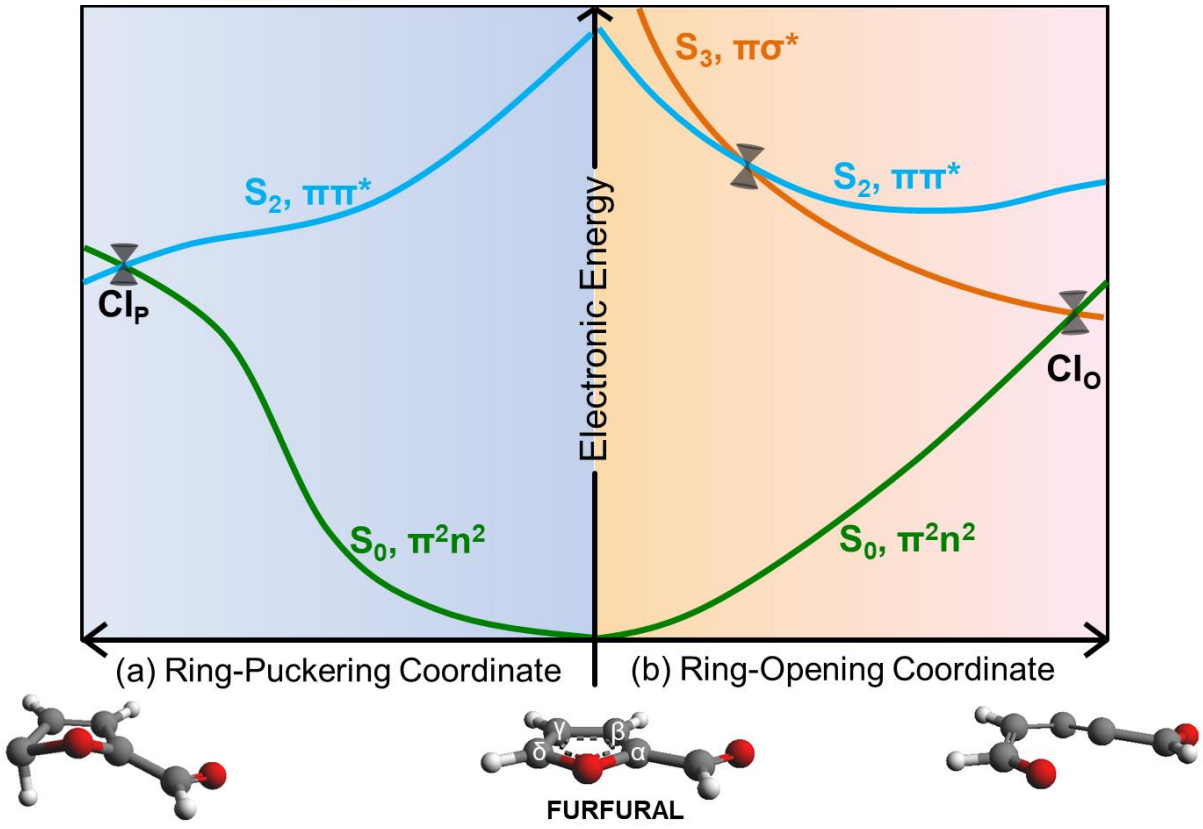

Figure 1: A schematic of the ultraviolet-induced photodynamics in furfural (also applicable to furan) shows the diabatic electronic states involved along the (a) ring-puckering and (b) ring-opening coordinates. S_n are defined at the Franck-Condon (FC) region of excitation for the electronic states concerned; S_0 ($\pi^2n^2\pi^{*0}$, ground-state), S_1 ($n\pi^*$, optically dark state, not shown), S_2 ($\pi\pi^*$, photoexcited state), S_3 ($\pi\sigma^*$). (It must be noted that the $\pi\sigma^*$ state lies higher than S_{15} for furan at the FC-point.[18] It is effectively S_3 for this schematic where the intermediate $\pi\pi^*$ and π-Rydberg states are ignored). The geometrical structures of the ground-state, ring-puckered (CI_P), and ring-opened (CI_O) conical intersections of furfural are shown at the bottom of the figure. (For detailed calculations, see Ref. 17)

Experimental detection of the ring-opened species is a challenge for many spectroscopic techniques.[10] Being a structural isomer of the ring-closed parent molecule, mass-gated photoionization

techniques are not particularly suited for ring-opening detection but work well to detect secondary unimolecular decay following internal (vibrational) excitation.[19,20] Experimental studies of the photoinduced ring-opened species often rely on reporter groups that have a changing spectral signature as the ring opens, such as a carbonyl-to-ketene transformation in 2-furanone and α-pyrone via time-resolved infrared spectroscopy.[21-23] The approach here utilizes ultrafast core-level spectroscopy to observe photoinduced dynamics in gas-phase photochemical reactions.[24-27] Time-resolved X-ray absorption spectroscopy is able to directly probe the frontier molecular orbitals of photoproducts such as radicals,[28-31] biradicals,[32] ring-open or ring-closed isomers,[24] and open-shell or closed-shell species[33-35] via fingerprint, core-to-LUMO (lowest unoccupied molecular orbital) and core-to-SOMO (singly-occupied molecular orbital) pre-edge resonances. The X-ray spectra of these frontier orbitals are unique and successfully predicted by theory, for comparison to experiment. The energetic separation of the near-edge transitions of different atomic sites by a few tens to hundreds of eV along with the broadband nature of table-top high harmonic generation offer a valuable method to sample large regions of the reaction coordinate from the perspective of individual constituent atoms or chemical groups. The element, orbital, and site-specificities of X-ray spectroscopy, when combined with time-resolved detection, constitute a universal probe of photoinduced dynamics.[36]

Methods

Femtosecond time-resolved X-ray absorption is performed in a recently upgraded table-top apparatus[24] that produces ultrashort (sub-60 fs), broadband soft X-ray pulses between 150 eV and 310 eV and covers the carbon K-edge (~284 eV). These soft X-ray pulses are used to probe the dynamics of photoexcited furfural over several picoseconds after ultraviolet excitation. A tunable optical parametric amplifier (1180-2600 nm; HE-TOPAS, Light Conversion) pumped by an ~90% split-off output of a Ti:sapphire laser (800 nm central wavelength, 12 W at 1 kHz, sub-35 fs pulse duration; Spitfire Ace, Spectra Physics) is used to produce high harmonics at a fundamental driving wavelength of 1320 nm (2.1 W at 1 kHz, sub-60 fs pulse duration). The beam is irised down, focussed by a 40-cm lens into a differentially-pumped, semi-infinite gas-cell containing helium (750-850 Torr), and the residual infrared is blocked by a 100 nm-thick aluminum filter. A toroidal mirror focuses the high harmonic, soft X-ray pulses into a sample cell (2 mm path length), which contains ~300 μm holes to

pass the laser beams and through which the vapors of furfural (Sigma Aldrich, sample heated at 80°C) are made to exit. Ultraviolet 266 nm pump pulses, produced by third-harmonic generation, are routed by a variable delay-stage (1 fs precision) and focused into the sample cell with a 40 cm focal length lens (~6 mW, sub-70 fs pulse duration, pump intensity of ~1.2×10^{11} W cm^{-2} at the pump-probe interaction region). The residual pump is blocked by a ~200 nm thick titanium foil, and the transmitted probe is dispersed by a 1200 lines/mm variable line-spaced, concave grating onto a CCD chip (1340×400 pixels, 20×20 μm pixel size; Princeton Instruments). An *in-situ* pump-probe cross-correlation is obtained by measurement of the ponderomotive shift of the core-excited Rydberg states of Argon, which sets the position for time zero and also the instrument response function (IRF) of the apparatus (90 fs, Figure S1). Further details may be found in the Supporting Information.

Ground-state, static X-ray absorption spectra of furfural are measured by referencing 64 high-harmonic transmission spectra (acquiring 1000 laser pulses per spectrum) in the presence (I) and absence (I_0) of the sample to obtain the optical density or absorbance, $A = -\log_{10}(I/I_0)$. Time-resolved differential X-ray absorption spectra (or X-ray transient absorption spectra) are obtained by measuring the X-ray absorbance of the sample in the presence (I_{on}) and absence (I_{off}) of the pump pulse at specified pump-probe time-delays while the sample vapors flow continuously. A typical pump-probe measurement averages 24 or 32 spectra (integrating 1000 laser pulses for each 'pump-on' and 'pump-off' configuration) over 60 pump-probe time delays between -450 fs and 10 ps, where positive time-delays denote the X-ray probe pulse arriving at the interaction region after the ultraviolet pump pulse. The differential absorbance (ΔA) for each time delay is then obtained as $-\log_{10}(I_{on}/I_{off})$ and added back to a scaled ground-state spectrum to derive the X-ray absorption spectrum of the photoexcited molecules alone. The reaction kinetics are calculated by taking single-energy lineouts of the key resonances over the measured time-delays and fitting the time-traces to exponential rise- or decay functions convolved with a Gaussian instrument response of fixed width (90 fs).

Previously reported electronic structure calculations[17] are used as a starting point for this work. All geometries are optimized on a complete active space self-consistent field (CASSCF) level of theory with 6-31G* as a basis set, except for the equilibrium geometry where coupled cluster CCSD(T) theory is used. Core-excited spectra are computed using the strongly-contracted n-electron

valence state perturbation theory (NEVPT2), a specialized version of complete active space perturbation theory (CASPT2) linked to the CASSCF reference states. The basis set employed is the correlation-consistent, core-valence triple-zeta basis set cc-pCVTZ which does not describe Rydberg orbitals particularly well, but is accurate for the frontier orbitals of π/π* character. For the sake of comparison, calculations are also carried out using time-dependent density functional theory TDDFT with basis sets incorporating diffuse functions. The NEVPT2 energies are found to depend strongly on a balanced description of the electron distribution around all atoms. This necessitated the use of different active spaces for the different molecular geometries. Consequently, all calculations are independently compared to the experimental spectra. At the FC point, an (8,7) active space is chosen, which comprises the whole π-space of furfural. At the conical intersections, the σ-orbitals of the elongated CO-bonds are added, which in the case of CI_P are delocalized within the π-space, and in case of CI_O are essential for the correct description of the electronic states. The spectra are simulated by Gaussian broadening (320 meV) of the NEVPT2 excitation energies and scaling with the transition dipole moments of the respective CASSCF reference states. Comparing the theoretical spectra to the experimental NEXAFS spectra, the absolute energy shifts needed for the NEVPT2 results are larger than for valence excitations. At the FC point (shift of ~6 eV), it still lies below the shift necessary for TDDFT (~10 eV). We primarily focus on the NEVPT2 results as TDDFT is not suited to describe the valence-excited states at the conical intersections. Also, the CIs and ring-open structures show many double excitations that are not described within TDDFT.

Results

The ground-state, near-edge X-ray absorption fine structure (NEXAFS) spectrum of furfural (solid black line with shaded-gray error bar, Figure 2) shows a strong peak at 286.4 eV and a low-energy shoulder at 285.1 eV. A NEXAFS calculation at the NEVPT2(8,7) level of theory indicates that the observed peaks correspond predominantly to 1s→π*(LUMO) resonances from several atoms. The unique chemical shifts of the inequivalent carbon atoms lend it a double-peak structure, as is also reported for furan.[37] Specifically, the peak at 286.4 eV corresponds to the core(1s)→LUMO(π*) transitions centered on the C_1 (yellow), C_4 (brown), and C_5 (red) atoms (see underlying colored-stick spectrum) whereas the shoulder mainly consists of a 1s(C_2, green)→π* transition and a 1s(C_3,

blue)→π* transition. These individual frequencies are presently not resolvable in the experiment and only a convolution of the computed stick spectrum with a Gaussian broadening equivalent to the spectrometer resolution (~320 meV, filled orange curve) can be directly compared with the experiment. The chemical shift of the carbon atoms C_1, C_4, and C_5 to higher energies in comparison to C_2 and C_3 is expected due to the proximity of the more electronegative oxygen heteroatom. The assignment is also consistent with the reported NEXAFS spectrum of furan, which contains two sets of inequivalent, chemically-shifted carbon atoms.[37,38] Figures S2-S3 show results obtained at other levels of theory (TDDFT) and for structural isomers of furfural. As NEXAFS spectra are mainly sensitive to the electronic structure, the contributions of nuclear structural isomers (cis / trans) to the measured spectra cannot be quantified.

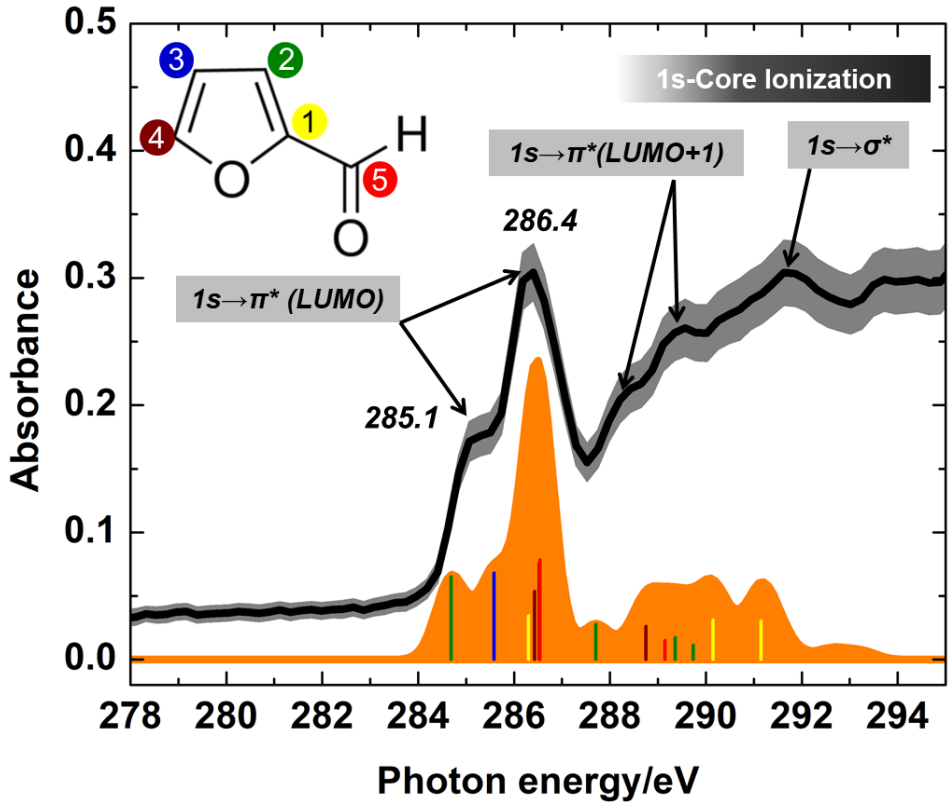

Figure 2: Experimentally measured, near-edge X-ray absorption fine-structure (NEXAFS) spectrum of furfural (solid black line, shaded gray region denotes 95% confidence interval limits) with the main peaks annotated. The calculated NEXAFS at the NEVPT2(8,7) level of theory is shown as a stick spectrum, color-coded as per the atom numbering scheme in the inset. The stick spectrum is uniformly offset by +6.4 eV to align with the experiment. The solid orange spectrum represents a convolution of the stick spectrum with a Gaussian broadening function equivalent to the spectrometer resolution of 0.32 eV. The calculation does not take into account the core-1s ionization and imposes an energy cut-off at 294 eV.

In the NEXAFS spectrum of furfural shown in Figure 2, the broad absorption peaks at 288.2 eV, 289.6 eV and at 291.6 eV, barely discernible over the rising edge that results from core-1s ionization, are mainly due to 1sπ*(LUMO+1) and 1sσ*(C-O) resonances.[37] Core-valence and core-Rydberg resonances that dominate this region of the spectrum are particularly difficult to reveal for two reasons; (i) coupling with the ionization continuum broadens these peaks due to a shape resonance and (ii) the 1s-core ionization significantly depletes the X-ray photon flux at these probe energies, which is evident through the larger error bars (shaded gray curve represents a 95% confidence interval) that accompany the data points measured over the carbon K-edge in comparison to the near-edge. These broad, high-energy peaks at the carbon K-edge are also reported in the NEXAFS spectrum of furan and share the same assignment.[37]

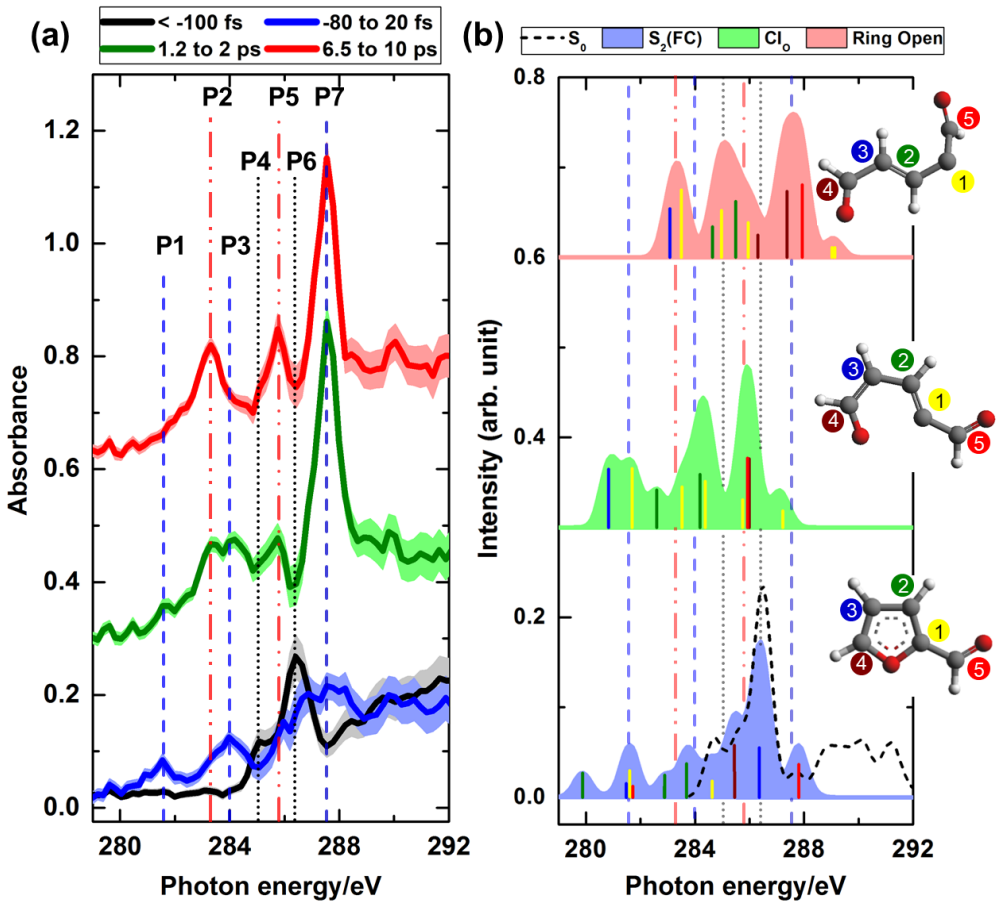

Figure 3: (a) NEXAFS spectra of photoexcited furfural derived from transient X-ray spectra measured at negative (< -100 fs, solid black line), short (-80 to 20 fs, solid blue), intermediate (1.2 to 2 ps, solid green), and long (6.5 to 10 ps, solid red) time delays. The spectra are vertically offset for clarity. The main peaks observed are annotated P1 through P7 in increasing order of energy. Shaded areas accompanying the solid lines represent 95% confidence interval limits. (b) Theoretical NEXAFS spectra of ground-state furfural (S_0, dashed black line, same as the solid orange spectrum in Figure 2), Franck-Condon excited region (S_2, filled light-blue), CI_O (filled light-green), and the ring-open

minimum energy structure (carbene, filled light-red), obtained by a convolution of the underlying, color-coded stick spectra. The peak positions of P1-P7 are also transferred to this panel for an easy reference to guide the eye. (Note that the calculations for the S_2 (FC) and CI_O points, shown here as a representation of the general reaction pathway may not be taken to directly correspond to the experimental traces as these are not stationary points, unlike the ring-opened carbene).

Figure 3(a) shows the measured evolution in the NEXAFS spectrum of furfural at representative time-delays following 266 nm photoexcitation. This includes time delays immediately following photoexcitation (-80 to 20 fs, solid blue), intermediate (1.2 to 2 ps, solid green) and long time-delays (7-10 ps), whereupon no further changes are detected in the transient absorption spectra. These pure 'pump-on' NEXAFS spectra are derived by adding the measured differential X-ray transient absorption spectra ('pump-on' minus 'pump-off' X-ray absorption signals) for each of the time-windows to a suitably scaled, experimental ground-state NEXAFS spectrum. The scaling factor is obtained by an estimation of the percentage of the ground-state molecules that are excited in the pump focal volume. This is found to be approximately 23%, based on the 266-nm absorption cross-section of furfural and the pump fluence (see Figure S4, which is linear over the range of pump fluence between 8 and 20 mJ/cm^2). Figure S5 shows the complete evolution of the transient absorption data over all timescales up to 10 ps and the corresponding, derived, pure 'pump-on' spectra are shown in Figure S6.

At time-delays ≤ -100 fs (solid black line, Figure 3a), the pump pulse arrives after the X-ray probe pulse, and this spectrum is therefore equivalent to the ground-state NEXAFS of furfural (Figure 2). At early times (-80 to 20 fs, blue trace), a depletion of the ground-state 1sπ*(LUMO) core-excited resonances is noted at 285.1 eV (P4) and 286.4 eV (P6) due to the π→π* optical excitation (vertical black dotted lines to guide the eye). These depletions occur immediately after photoexcitation (50±40 fs, Figure 4), as revealed by a temporal lineout taken at P6, and show a constant amplitude up until the longest measured time-delays (10 ps). Three new, weak absorption peaks (vertical blue dashed lines to guide the eye) are also identified in the blue trace, at 281.6 eV (P1), 284.0 eV (P3), and 287.5 eV (P7). P1 and P3, which appear lower in energy than the ground-state NEXAFS peaks of furfural at P4 and P6, must correspond to the transitions of a 1s-core electron into the hole produced in the singly-occupied π-orbital resulting from the valence excitation. Specifically, these represent chemically shifted, core-to-(singly-occupied) HOMO transitions in photoexcited furfural. It must be noted that

these spectral features that appear as 'single' peaks actually contain a number of underlying core-to-valence resonances from inequivalent carbon atoms, which cannot be spectrally resolved (see representative stick spectra, Figure 3b). Interestingly, a minor, broad depletion is also noted in the region between 291 and 292 eV which represents a decreased absorption of the 1sσ* resonance. As the σ* orbital is not involved in the optical excitation, a depletion in the 1sσ* resonance at early times may possibly arise from non-adiabatic population transfer from the ππ* to the πσ* state, as required in a ring-opening process. However, the low probe-photon counts above the absorption edge, together with the broad widths of the absorption peaks in this region render a concrete assignment to ultrafast non-adiabatic dynamics far from unambiguous at this stage.

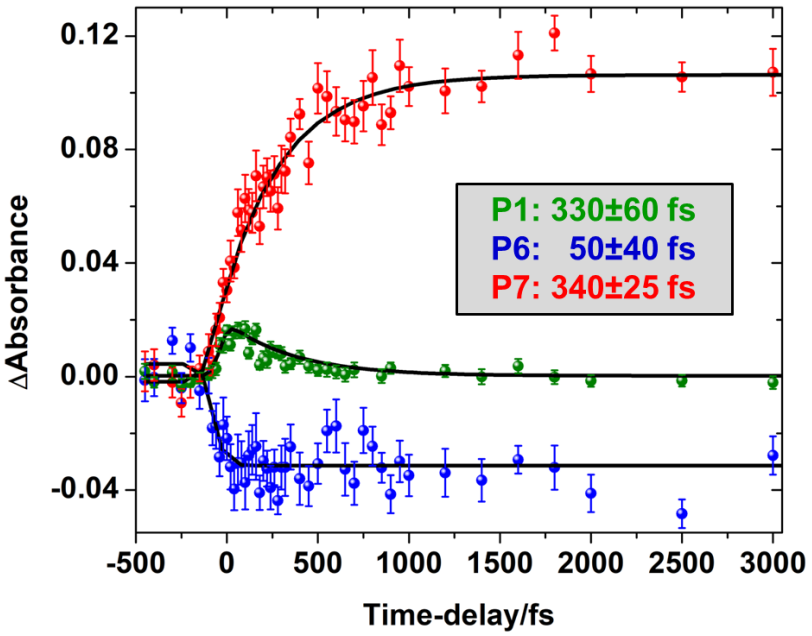

Figure 4: Temporal evolutions of P1, P6, and P7 are characterized by exponential time-constants indicated in the inset. The peaks are fitted to an exponential rise (P6 and P7) or decay (P1), convolved with a Gaussian instrument response function of fixed width (90 fs). The error bars accompanying the measured data points represent 95% confidence intervals and the error bars in the quoted time-constants represent one standard error in the least-squares fitting.

All three peaks (P1, P3, and P7) are found to grow in amplitude for several hundreds of femtoseconds (Figures S5-S6). As the photochemical reaction proceeds to intermediate time-delays (> 1 ps, solid green line in Figure 3a), P7 continues to grow whereas the amplitudes of P1 and P3 gradually decrease with the concomitant appearance of two new peaks, P2 (283.3 eV) and P5 (285.8 eV) (red dot-dashed lines). The kinetics of P1 (Figure 4) reveals an exponential decay constant of

330±60 fs which represents the excited-state lifetime. Finally, at the longest measured time-delays (7-10 ps, solid red line in Figure 3a), only three new peaks remain at 283.3 eV (P2), 285.8 eV (P5), and 287.5 eV (P7). Of these, the position of P2 is strikingly similar to a core-1s transition into a non-bonding (2p) orbital of a carbon atom, and it has been identified earlier in the soft X-ray absorption spectra of organic radicals.[28, 32, 39] Therefore, it is assigned to a carbon 1s→2p transition in ring-opened furfural. A 266-nm power-dependence study of the most intense peak (P7, 287.5 eV) shows a linear scaling with a slope of near-unity and is consistent with a one-photon excitation process (Figure S4). This peak rises with a time-constant of 340±25 fs, as shown in Figure 4, and its kinetics are similar to that of P2 (350±50 fs, Figure S7). Thus, these peaks are most likely representative of the same final state.

Discussion

The formation of a vibrationally-hot furfural molecule from non-reactive internal conversion to the ground-state is expected to lead to a broadening of the ground-state NEXAFS peaks and partial or full recovery of the parent depletion at longer time-delays, depending on the branching fraction. In the ring-opening reaction of 1,3-cyclohexadiene (CHD), where a significant percentage (~60%) of the molecules internally convert to the ground state, non-adiabatic molecular dynamics simulations were used to obtain the NEXAFS of the vibrationally-hot CHD at the carbon K-edge.[24] The simulations predicted a decrease in the oscillator strength and increase in the width (due to vibrational broadening), but no significant peak shifts of the 1sπ* electronic resonance of hot CHD compared to a Boltzmann distribution of CHD in the ground-state at 300 K. In a NEXAFS study of thymine photophysics (266 nm) at the oxygen K-edge, internal conversion to the ground state manifests as a recovery of the ground-state depletion.[40] Formation of an open-chain radical intermediate in furfural, on the other hand, is expected to result in new, fingerprint core (1s) to frontier-orbital (2p,π*) resonances, with large energy separations (~eV) with respect to the parent molecule.

Both the ring-opening and ring-puckering co-ordinates are expected to involve low-frequency C-O-C out-of-plane vibrations, C-O stretching as well as in-plane bending modes. The internal energy gets distributed over multiple vibrational modes as a result of non-adiabatic dynamics. The vibrational energy per normal mode (in the limit of statistical partitioning of the excess energy) is only a couple

of hundred meV at best. This is not only comparable to the carbon 1s-core-hole broadening widths (~100 meV) but also well within the spectral resolution of the instrument (~340 meV). At present, the experiment is not sensitive to intramolecular vibrational energy redistribution. This is because the excess vibrational energy per normal mode is small (~200 meV) in comparison to the NEXAFS spectral resolution (core-hole lifetime of ~100 meV plus instrumental resolution of ~320 meV).

To gain insights into the reaction pathway of photoexcited furfural, the NEXAFS spectra are simulated for representative points on the potential energy surface (Figures 3b and S8). This includes the photoexcited Franck-Condon region (filled blue curve, Figure 3b), CI_O (filled green) as well as the ground state of the ring-opened, minimum energy structure (carbene, filled red). It must be noted that our experiment is not uniquely sensitive to wavepacket dynamics at FC and CI points that require few-femtosecond temporal resolution;[41] however, these are included in Figure 3b for a representation of the overall reaction pathway. The computed NEXAFS spectrum for the FC-region in the optically bright S_2 state (where only the electronic structure changes at the frozen ground-state molecular geometry) agrees remarkably well with the observed early time-delay spectrum, in regard to the positions of P1 and P3 (within instrumental resolution). As mentioned earlier, these peaks arise mainly from a core-1s electronic excitation into the hole left in the HOMO of the parent molecule upon ultraviolet excitation. The computed peak at 279.9 eV for the FC-point is not observed as a distinct peak in the experiment but rather as a low energy tail (see comparisons of the differential absorption spectra, Figure S9). The computed spectrum of the CI_O fits the experimental spectrum between 120 and 200 fs (Figure S9) very well, suggesting that a distribution of opened structures likely dominate the early-time NEXAFS spectra.

Most importantly, the positions of P2 and P7 observed at the longest time delays are in excellent agreement with the computed NEXAFS of an open-chain carbene intermediate (filled red curve, Figure 3b) which is found to be a minimum energy structure for ring-opened furfural. P2 and P5 mainly represent the chemically-shifted, core-to-2p (LUMO) and core-to-π* (LUMO+1) resonances of the ring-open isomer, whereas P7 is predominantly core-to-π* (LUMO+1) and core-to-π* (LUMO+2) resonances. The minor discrepancy in the experimental and theoretical positions of P5 could be due to the fact that the computed peak center overlaps with a ground-state depletion (P4),

which might shift the observed P5 peak center to slightly higher energies. A previous study on the ultrafast relaxation dynamics of furan tentatively assigned the observed photoelectron bands to the formation of carbenes.[15] A ring opened furfural is also implicated in pyrolysis measurements[42] and hypothesized to involve a carbene intermediate in the pyrolysis of furan[16] and 2-methyl furan.[43] Herein, the unique sensitivity of NEXAFS spectroscopy to electronic structure provides direct evidence for photochemical ring-opening in furfural via a carbene intermediate, through core electronic transitions into its unoccupied, frontier molecular orbitals. A biradical structure (see Figure S10 and related note) arising from homolytic C-O bond fission could also be computationally identified in a few trajectories in the ring-opening of furfural; however, it does not correspond to a minimum energy structure.

The key photophysics accompanying the photoinduced ring-opening reaction and associated timescales are illustrated in Figure 4. The depletion of the 1sπ* (LUMO) resonance at P6 sets in sharply near time zero with a time-constant of ~50±40 fs, reaches a plateau by 200 fs and shows no subsequent recovery up to the longest measured timescales (~10 ps), indicating that non-reactive internal conversion to the ground-state does not occur or is only a minor channel (within one standard error of the fitted P6 amplitude which corresponds to ~5%). If the return to the ground state leads to vibrationally broadened features (~200 meV, by analogy to theoretical results reported for CHD),[24] the integrated peak area may be taken into account to estimate repopulation of S_0. This procedure returns a standard error of ~8% with respect to the mean integrated differential absorbance (between 286 eV and 287 eV, Figure S11). A conservative upper limit for the return to the ground state is further derived by the effect of the vibrational broadening expected in the hot ground state (~200 meV) on the measured peak width of P6 in ground state furfural (0.95 eV, Figure S12), which is ~10% when weighted by the instrumental resolution. The best upper estimate of S_0 repopulation is therefore 8% based on the signal to noise ratio in the integrated differential absorbance, and is adjusted to 10% due to anticipated vibrational broadening. Previously reported on-the-fly dynamics of furfural averaged over 100 trajectories, initiated in the electronic state nearest to the HOMO-LUMO energy gap (labelled S_4 in that paper but S_2 according to Figure 1), indicate little ground-state population recovery (< 15%) up to 500 fs.[17] Time-resolved infrared measurements of the closely-

related molecule, 2-furanone, in acetonitrile at 225 nm, also reveal prompt ring-opening on a sub-1 ps timescale with less than 10% of the molecules reported to undergo internal conversion to the ground electronic state.[22] With improved flux in table-top soft X-ray setups, independent quantitative estimates of branching fractions in photochemical reactions will be feasible in the near future. The significantly low fraction of return to the ground state and lack of other features over the many picosecond timescales suggest that ring opening is the predominant photodynamical pathway in gaseous furfural at 266 nm and likely involves a carbene intermediate.

The ultrafast rise of P2 (350±50 fs) and P7 (340±25 fs) (Figures 4 and S7), characterized by similar time-constants, is indicative of these peaks originating from the same ring-opened photoproduct. This sub-400 fs ring-opening originates on the barrierless excited state surface since any ring opening in the ground state is expected to be significantly slower.[44] The products are formed with high internal excitation and may undergo further isomerization (via H-atom migration) or even fragmentation, which can be better probed in the future with higher NEXAFS spectral resolution and by sampling longer time-delays. P1, characterized by an ultrafast rise (73±20 fs with respect to the onset of ground-state depletion) and decay (330±60 fs), is indicative of an intermediate photoexcited state that rapidly decays into the product. The temporal behavior of P1 in Figure 4 is plotted after subtraction of the contribution from the low-energy wing of P2 in the long-delay limit differential absorption signals in this region (Figure S13). The quoted error bars for the time-constants correspond to one standard-error from the least-squares fitting routine. Future experiments with even shorter pulses are likely to reveal the dynamics of the intermediate excited states and passage through conical intersections. Complementary experiments at the oxygen K-edge (~543 eV) can also enable an alternative view of the photochemical reaction pathway via a much simplified 1s-core spectrum of the heteroatom.[41]

Conclusion

Femtosecond X-ray transient absorption spectroscopy is a powerful technique to unravel photoinduced isomerization in ring compounds via changes in fingerprint core-to-unoccupied frontier orbital resonances. Carbon K-edge spectroscopy of the 266-nm induced photochemistry of furfural provides direct evidence for an ultrafast ring-opening reaction on a ~350-fs timescale. Internal

conversion to the ground-state is ruled out to within 10%, from the negligible recovery of the parent 1sπ* resonance at 286.4 eV and expected vibrational broadening effects. No particular X-ray spectral signatures are obtained to specifically rule out the ring puckering channel; however, the estimates of internal conversion to the ground state indirectly set an upper limit for this pathway. While the NEXAFS spectra are mostly sensitive to electronic structure changes, improvement in high harmonic generation efficiencies and flux above the carbon K-edge will enable tracking changes in the nuclear geometry through the extended X-ray absorption fine structure (EXAFS).[45] These experimental results lay an initial groundwork for the application of core-level spectroscopy to a broad class of ring-opening photochemical reactions in organic heterocycles, such as epoxide ring opening in organic aerosols, radical chain-initiation steps in ring-opening polymerization reactions, etc. An increase in the temporal resolution via pump (266 nm) pulse compression and using isolated attosecond pulses at the carbon K-edge will open exciting new possibilities of probing wavepacket dynamics at conical intersections in the future.[46,47]

Supporting Information

Instrument response; Comparisons of experimental NEXAFS spectra with theory; Pump-power dependence study; Transient absorption data and associated temporal evolution over the full time-window probed.

Author Information

Corresponding Author

srl@berkeley.edu

Present addresses

[5]School of Chemistry, University of Bristol, Bristol BS8 1TH, United Kingdom

[6]Paul Scherrer Institute, 5232 Villigen, Switzerland

Notes

The authors declare no competing financial interest.

Acknowledgements

This research work, A.B., Z.Y., and T.X. were supported by the U.S. Department of Energy, Office of Science, Office of Basic Energy Sciences (Contract No. DE-AC02-05CH11231), the gas phase chemical physics program through the Chemical Sciences Division of Lawrence Berkeley National Laboratory. The apparatus was partially funded by a NSF ERC, EUV Science and Technology, under a previously completed grant (No. EEC-0310717). K.S. was supported by a Peter Paul Ewald Fellowship from the Volkswagen Foundation. R.D.V.R. and S.O. acknowledge financial support by the Deutsche Forschungsgemeinschaft through SFB749 and the excellence cluster Munich-Centre for Advanced Photonics (MAP).

References

1. de Melo, J. S.; Elisei, F.; Becker, R. S. Photophysical studies of mixed furan, pyrrole, and thiophene-containing oligomers with three and five rings. *J Chem Phys* **2002,** *117* (9), 4428-4435.

2. Woo, C. H.; Beaujuge, P. M.; Holcombe, T. W.; Lee, O. P.; Frechet, J. M. J. Incorporation of furan into low band-gap polymers for efficient solar cells. *J Am Chem Soc* **2010,** *132* (44), 15547-15549.

3. Li, R. Z.; Lv, X. J.; Shi, D.; Zhou, D. F.; Cheng, Y. M.; Zhang, G. L.; Wang, P. Dye-sensitized solar cells based on organic sensitizers with different conjugated linkers: furan, bifuran, thiophene, bithiophene, selenophene, and biselenophene. *J Phys Chem C* **2009,** *113* (17), 7469-7479.

4. Tsuji, H.; Nakamura, E. Design and functions of semiconducting fused polycyclic furans for optoelectronic applications. *Accounts Chem Res* **2017,** *50* (2), 396-406.

5. Meotti, F. C.; Silva, D. O.; dos Santos, A. R. S.; Zeni, G.; Rocha, J. B. T.; Nogueira, C. W. Thiophenes and furans derivatives: a new class of potential pharmacological agents. *Environ Toxicol Phar* **2003,** *15* (1), 37-44.

6. Atkinson, R.; Arey, J. Atmospheric chemistry of biogenic organic compounds. *Accounts Chem Res* **1998,** *31* (9), 574-583.

7. Lohmann, R.; Jones, K. C. Dioxins and furans in air and deposition: A review of levels, behaviour and processes. *Sci Total Environ* **1998,** *219* (1), 53-81.

8. Eldeeb, M. A.; Akih-Kumgeh, B. Reactivity trends in furan and alkyl furan combustion. *Energ Fuel* **2014,** *28* (10), 6618-6626.

9. Roman-Leshkov, Y.; Barrett, C. J.; Liu, Z. Y.; Dumesic, J. A. Production of dimethylfuran for liquid fuels from biomass-derived carbohydrates. *Nature* **2007,** *447* (7147), 982-986.

10. Ashfold, M. N. R.; Bain, M.; Hansen, C. S.; Ingle, R. A.; Karsili, T. N. V.; Marchetti, B.; Murdock, D. Exploring the dynamics of the photoinduced ring-opening of heterocyclic molecules. *J Phys Chem Lett* **2017,** *8* (14), 3440-3451.

11. Lange, J. P.; van der Heide, E.; van Buijtenen, J.; Price, R. Furfural-A promising platform for lignocellulosic biofuels. *Chemsuschem* **2012,** *5* (1), 150-166.

12. Zhao, X. C.; Wang, L. M. Atmospheric Oxidation Mechanism of Furfural Initiated by Hydroxyl Radicals. *J Phys Chem A* **2017,** *121* (17), 3247-3253.

13. Fuji, T.; Suzuki, Y. I.; Horio, T.; Suzuki, T.; Mitric, R.; Werner, U.; Bonacic-Koutecky, V. Ultrafast photodynamics of furan. *J Chem Phys* **2010,** *133* (23), 044302.

14. Spesyvtsev, R.; Horio, T.; Suzuki, Y. I.; Suzuki, T. Excited-state dynamics of furan studied by sub-20-fs time-resolved photoelectron imaging using 159-nm pulses. *J Chem Phys* **2015,** *143* (1), 014302.

15. Liu, Y. Z.; Knopp, G.; Qin, C. C.; Gerber, T. Tracking ultrafast relaxation dynamics of furan by femtosecond photoelectron imaging. *Chem Phys* **2015,** *446*, 142-147.

16. Urness, K. N.; Guan, Q.; Golan, A.; Daily, J. W.; Nimlos, M. R.; Stanton, J. F.; Ahmed, M.; Ellison, G. B. Pyrolysis of furan in a microreactor. *J Chem Phys* **2013,** *139*, 124305.

17. Oesterling, S.; Schalk, O.; Geng, T.; Thomas, R. D.; Hansson, T.; de Vivie-Riedle, R. Substituent effects on the relaxation dynamics of furan, furfural and beta-furfural: a combined theoretical and experimental approach. *Phys Chem Chem Phys* **2017,** *19* (3), 2025-2035.

18. Gavrilov, N.; Salzmann, S.; Marian, C. M. Deactivation via ring opening: A quantum chemical study of the excited states of furan and comparison to thiophene. *Chem Phys* **2008,** *349* (1-3), 269-277.

19. Sorkhabi, O.; Qi, F.; Rizvi, A. H.; Suits, A. G. Ultraviolet photodissociation of furan probed by tunable synchrotron radiation. *J Chem Phys* **1999,** *111* (1), 100-107.

20. Shibata, T.; Li, H. Y.; Katayanagi, H.; Suzuki, T. Dissociation of metastable CH3CO radical observed by subpicosecond time-clocked photofragment imaging. *J Phys Chem A* **1998,** *102* (21), 3643-3647.

21. Breda, S.; Reva, I.; Fausto, R. UV-induced unimolecular photochemistry of 2(5H)-furanone and 2(5H)-thiophenone isolated in low temperature inert matrices. *Vib Spectrosc* **2009,** *50* (1), 57-67.

22. Murdock, D.; Harris, S. J.; Luke, J.; Grubb, M. P.; Orr-Ewing, A. J.; Ashfold, M. N. R. Transient UV pump-IR probe investigation of heterocyclic ring-opening dynamics in the solution phase: the role played by n sigma* states in the photoinduced reactions of thiophenone and furanone. *Phys Chem Chem Phys* **2014,** *16* (39), 21271-21279.

456 23. Murdock, D.; Clark, I. P.; Ashfold, M. N. R. Probing photochemically and thermally induced
457 isomerization reactions in alpha-pyrone. *J Phys Chem A* **2016,** *120* (37), 7249-7254.
458 24. Attar, A. R.; Bhattacherjee, A.; Pemmaraju, C. D.; Schnorr, K.; Closser, K. D.; Prendergast,
459 D.; Leone, S. R. Femtosecond x-ray spectroscopy of an electrocyclic ring-opening reaction. *Science*
460 **2017,** *356* (6333), 54-58.
461 25. Bhattacherjee, A.; Das Pemmaraju, C.; Schnorr, K.; Attar, A. R.; Leone, S. R. Ultrafast
462 intersystem crossing in acetylacetone via femtosecond X-ray transient absorption at the carbon K-
463 edge. *J Am Chem Soc* **2017,** *139* (46), 16576-16583.
464 26. Bhattacherjee, A.; Attar, A. R.; Leone, S. R. Transition state region in the A-Band
465 photodissociation of allyl iodide-A femtosecond extreme ultraviolet transient absorption study. *J*
466 *Chem Phys* **2016,** *144* (12), 124311.
467 27. Attar, A. R.; Bhattacherjee, A.; Leone, S. R. Direct observation of the transition-state region
468 in the photodissociation of CH3I by femtosecond extreme ultraviolet transient absorption
469 spectroscopy. *J Phys Chem Lett* **2015,** *6* (24), 5072-5077.
470 28. Alagia, M.; Bodo, E.; Decleva, P.; Falcinelli, S.; Ponzi, A.; Richter, R.; Stranges, S. The soft
471 X-ray absorption spectrum of the allyl free radical. *Phys Chem Chem Phys* **2013,** *15* (4), 1310-1318.
472 29. Ekstrom, U.; Carravetta, V.; Alagia, M.; Lavollee, M.; Richter, R.; Bolcato, C.; Stranges, S.
473 The umbrella motion of core-excited CH3 and CD3 methyl radicals. *J Chem Phys* **2008,** *128* (4),
474 044302.
475 30. Attar, A. R.; Piticco, L.; Leone, S. R. Core-to-valence spectroscopic detection of the CH2Br
476 radical and element-specific femtosecond photodissociation dynamics of CH2IBr. *J Chem Phys* **2014,**
477 *141* (16), 164308.
478 31. Ochmann, M.; von Ahnen, I.; Cordones, A. A.; Hussain, A.; Lee, J. H.; Hong, K.; Adamczyk,
479 K.; Vendrell, O.; Kim, T. K.; Schoenlein, R. W.; Huse, N. Light-induced radical formation and
480 isomerization of an aromatic thiol in solution followed by time-resolved X-ray absorption
481 spectroscopy at the sulfur K-edge. *J Am Chem Soc* **2017,** *139* (13), 4797-4804.

32. Kanai, K.; Noda, Y.; Kato, K.; Kubo, T.; Iketaki, K.; Shimizu, A.; Ouchi, Y.; Nakasuji, K.; Seki, K. Electronic structure of delocalized singlet biradical Ph-2-IDPL solid film. *Phys Chem Chem Phys* **2010,** *12* (39), 12570-12577.

33. Ruzankin, S. P.; Zilberberg, I.; Zhidomirov, G. M. Closed and open-shell atomic oxygen on silver: two distinct patterns of the O-1s binding energy and X-ray absorption 0 K-edge spectra as revealed by density functional theory. *Res Chem Intermediat* **2004,** *30* (1), 75-85.

34. Otero, E.; Kosugi, N.; Urquhart, S. G. Strong double excitation and open-shell features in the near-edge x-ray absorption fine structure spectroscopy of ferrocene and ferrocenium compounds. *J Chem Phys* **2009,** *131* (11), 114313.

35. Nocton, G.; Booth, C. H.; Maron, L.; Ricard, L.; Andersen, R. A. Carbon-hydrogen bond breaking and making in the open-shell singlet molecule Cp*Yb-2(4,7-Me(2)phen). *Organometallics* **2014,** *33* (23), 6819-6829.

36. Bressler, C.; Chergui, M. Ultrafast X-ray absorption spectroscopy. *Chem Rev* **2004,** *104* (4), 1781-1812.

37. Newbury, D. C.; Ishii, I.; Hitchcock, A. P. Inner shell electron-energy loss spectroscopy of some heterocyclic molecules. *Can J Chem* **1986,** *64* (6), 1145-1155.

38. Solomon, J. L.; Madix, R. J.; Stohr, J. Orientation and absolute coverage of furan and 2,5-dihydrofuran on Ag(110) determined by near edge X-Ray absorption fine-structure and X-ray photoelectron-spectroscopy. *J Chem Phys* **1991,** *94* (5), 4012-4023.

39. Okajima, T.; Fujimoto, H.; Sumitomo, M.; Araki, T.; Ito, E.; Ishii, H.; Ouchi, Y.; Seki, K. Soft X-ray absorption spectra of the lithium phthalocyanine radical. *Surf Rev Lett* **2002,** *9* (1), 441-446.

40. Wolf, T. J. A.; Myhre, R. H.; Cryan, J. P.; Coriani, S.; Squibb, R. J.; Battistoni, A.; Berrah, N.; Bostedt, C.; Bucksbaum, P.; Coslovich, G.; Feifel, R.; Gaffney, K. J.; Grilj, J.; Martinez, T. J.; Miyabe, S.; Moeller, S. P.; Mucke, M.; Natan, A.; Obaid, R.; Osipov, T.; Plekan, O.; Wang, S.; Koch, H.; Guhr, M. Probing ultrafast pi pi*/n pi* internal conversion in organic chromophores via K-edge resonant absorption. *Nat Commun* **2017,** *8*, 29.

41. Hua, W. J.; Oesterling, S.; Biggs, J. D.; Zhang, Y.; Ando, H.; de Vivie-Riedle, R.; Fingerhut, B. P.; Mukamel, S. Monitoring conical intersections in the ring opening of furan by attosecond stimulated X-ray Raman spectroscopy. *Struct Dynam* **2016,** *3* (2), 023601.

42. Vasiliou, A. K.; Kim, J. H.; Ormond, T. K.; Piech, K. M.; Urness, K. N.; Scheer, A. M.; Robichaud, D. J.; Mukarakate, C.; Nimlos, M. R.; Daily, J. W.; Guan, Q.; Carstensen, H. H.; Ellison, G. B. Biomass pyrolysis: thermal decomposition mechanisms of furfural and benzaldehyde. *J Chem Phys* **2013,** *139* (10), 104310.

43. Tranter, R. S.; Lynch, P. T.; Randazzo, J. B.; Lockhart, J. P. A.; Chen, X.; Goldsmith, C. F. High temperature pyrolysis of 2-methyl furan. *Phys Chem Chem Phys* **2018,** *20* (16), 10826-10837.

44. Qi, F.; Sorkhabi, O.; Rizvi, A. H.; Suits, A. G. 193 nm photodissociation of thiophene probed using synchrotron radiation. *J Phys Chem A* **1999,** *103* (42), 8351-8358.

45. Teo, B. K. Chemical applications of extended X-ray absorption fine-structure (Exafs) spectroscopy. *Accounts Chem Res* **1980,** *13* (11), 412-419.

46. Silva, F.; Teichmann, S. M.; Cousin, S. L.; Hemmer, M.; Biegert, J. Spatiotemporal isolation of attosecond soft X-ray pulses in the water window. *Nat Commun* **2015,** *6*, 6611.

47. Li, J.; Ren, X. M.; Yin, Y. C.; Zhao, K.; Chew, A.; Cheng, Y.; Cunningham, E.; Wang, Y.; Hu, S. Y.; Wu, Y.; Chini, M.; Chang, Z. H. 53-attosecond X-ray pulses reach the carbon K-edge. *Nat Commun* **2017,** *8*, 186.

528 **Table of Contents Graphic**

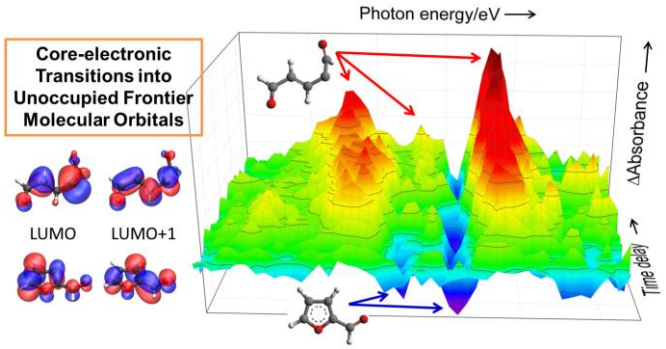

529